Int. J. Electrochem. Sci., 16 **(2021)** Article ID: 210843, doi: 10.20964/2021.08.46

International Journal of
ELECTROCHEMICAL
SCIENCE
www.electrochemsci.org

Preparation of an Electrochemical Sensor for Rapid Detection of Lead(II) in Blueberries

Hong Wu[1,*], *Sainan Qiao*[2], *Ning Zhang*[2] *and Yali Zhang*[1]

[1] College of Tourism and Hotel Management, Shanxi Technology and Business College, Taiyuan, Shanxi, 030000 China
[2] Department of Nursing and Health Management, Shijiazhuang Vocational College of Finance & Economics, Shijiazhuang, Hebei, 050061, China
[*]E-mail: hongwu_197778@163.com

Received: 15 April 2021 / *Accepted:* 4 June 2021 / *Published:* 30 June 2021

Blueberries tend to accumulate lead ions in the plant tissue for the reason that they are grown in acidic soil. The detection of lead ions in blueberries is a very important research objective in the field of food safety. In this work, a highly fast technique for electrochemical analysis was proposed. Nitrogen-doped carbon nanospheres were synthesized for the surface modification of glassy carbon electrodes, and the modified electrodes exhibited a sensitive response to lead ions. By optimizing the potential increments, pulse amplitude, pulse width, accumulation potential and accumulation time, this method can detect lead ions in the range of 10 nM-4 μM with the detection limit calculated to be 1.05 nM. In addition, the proposed electrochemical analysis has been successfully adopted to detect lead ions in blueberry samples.

Keywords: Lead ions; Electrochemical sensor; Analytical method; Blueberry; Nitrogen-doped carbon sphere

1. INTRODUCTION

Heavy metals are metallic elements with a relative density greater than 4.0 and are naturally found in rocks of the earth's crust. Human industrial and commercial activities result in environmental pollution by heavy metals, including air, water and soil pollution[1–3], among which soil heavy metal pollution is a worldwide problem. Heavy metals are presented in the soil in many forms, and the activity of heavy metals varies depending on the form in which they exist [4–8]. Heavy metals are most active in the water-soluble state and the exchange state, in which they can be easily absorbed by plants and are highly toxic [9–14].

Lead is one of the constituent elements of the earth's crust, and lead in soil under natural conditions mainly comes from the soil-forming matrix. The average background content of lead in the world soil is 15.25 mg/kg, and with the development of industry, the annual consumption of lead in the world is up to 4 million tons, most of which are not recycled and cause different forms of pollution to the environment [15–19]. Lead mainly exists in soil as $PbCO_3$, $PbSO_4$, $Pb(OH)_2$ and other divalent insoluble compounds. The strong adsorption capacity of soil makes it difficult to be absorbed by plants, thus the toxicity of lead is suppressed. However, when the pH of the soil is lowered, some of the $Pb(CO)_3$ in the soil is converted into Pb^{2+} which can be absorbed by plants with the uptake of Pb mainly existing in the roots. The low concentration of Pb can promote the growth of some plants, while the high Pb inhibits the normal growth and metabolism of plants and even has a lethal effect [20–22].

Lead damage is mainly manifested by accumulation in plants, shrinkage of seedlings, retardation of plant growth and reduction of crop yield. The tolerance level of lead in different plant species varies greatly [23–25]. Blueberry is a genus of lingonberry in the Rhododendron family. The fruit of blueberry can be eaten fresh and also processed into dried fruit, jam, juice as well as fruit wine. Blueberries were native to Canada and the western United States, with a great number of varieties and about 400 species worldwide. Blueberries vary in environmental requirements. The pH of the soil for blueberry cultivation ranges from 4.0-5.5 and the optimum pH is 4.3-4.8 [26], which directly affects the growth condition and fruit yield of blueberry [27,28]. Therefore, it is of great importance to test for lead in blueberries.

The detection of heavy metals in plants should be preceded by appropriate processing, such as dehulling, crushing, grinding, homogenizing, etc. The steps include filtration, centrifugation, dissolution and purification, followed by digestion of the sample and the methods of digestion are usually dry ashing, wet digestion and closed digestion [29–31]. The detection methods are atomic absorption spectrometry, graphite furnace atomic absorption, flame atomic absorption and inductively coupled plasma mass spectrometry. However, these analytical methods often require large instruments and a long time of operation. In contrast, electrochemical sensors are much faster and simpler, which have been widely used in food detection, requiring sensitive detection electrodes [32–34]. The preparation of suitable detection electrodes is the main research direction in this field.

Carbon nanosphere material is a type of nanomaterials, and is one of the isomers of carbon in macroscopic level, with a more extensive application research. Carbon nanosphere materials are spherical in microstructure, and their mechanical structure determines a high specific surface area [35–37], while their chemical composition determines their biocompatibility. Carbon nanosphere materials, with a certain adsorption effect and a smaller size, have an ability to transfer electrons compared to other non-carbon materials. However, some non-hydrophilic properties that are determined by the elemental composition and mechanical structure of carbon nanosphere materials greatly hinder their application in aqueous systems. The doping of exotic elements can significantly improve carbon materials' structure and electrical conductivity, among which nitrogen doping has become a hot research topic. Nitrogen is adjacent to carbon in the periodic table, and its atomic radius is close to that of carbon, thus the doping of nitrogen atoms can minimize the distortion of the original lattice of carbon materials [38–40]. After being doped into carbon materials, nitrogen atoms play the role of loaded electrons, which increases the charge density of the materials, thus increasing the electrical conductivity. Meanwhile, the doping of nitrogen atoms can also improve the water solubility of the materials, and their ability to bind

to metal ions can facilitate the disperse of metal ions to the surface of the carbon materials. In this work, the glassy carbon electrode (GCE) was surface-modified with nitrogen-doped carbon nanospheres and the modified electrode was adopted to detect lead ions. This sensor has been successfully applied to the detection of lead ions in blueberries.

2. MATERIALS AND METHODS

All reagents were analytical grade and used without further purification. 16 mL of ethanol was mixed with 40 mL of water, and 0.6 mL of 1-butyl-3-methylimidazole hydroxide ionic liquid was added. The mixture was stirred for 1 h. Afterwards, 0.4 g of resorcinol was added to the solution which was stirred until completely dissolved, and 0.56 mL of formaldehyde solution (37 wt%) was added and stirred at 30°C for 24 h. The mixture was transferred to a hydrothermal kettle and reacted at 100°C for 24 h. After centrifugation and washing, the mixture was dried at 100°C, after which the powder was carbonized in nitrogen atmosphere and heated up to 350°C at 1°C/min for 2 h. The powder was heated up to 600°C at 1°C/min for 4 h and cooled to room temperature to obtain nitrogen-doped carbon spheres (denoted as NC).

The surface of GCE was oxidized to produce various oxygen-containing groups including alcohols, phenols, carboxyl groups, anhydrides, etc., resulting in a loss of reproducibility, stability, and sensitivity of the electrode. The GCE was first polished with sandpaper, followed by a polishing to a mirror surface with 0.3 μm and 0.05 μm diameter aluminum trioxide powder on a chamois, and was moved to an ultrasonic water bath for 3 min. After thorough washing, the electrode was repeatedly scanned by cyclic voltammetry in 1 M H_2SO_4 solution at -0.8 V to 0.8 V until the curve was stable. For GCE modification, NC dispersion (dispersed in a chitosan solution) was drop coated on the GCE surface and dried naturally. All electrochemical measurements were carried out in a CHI 820D working station. A Ag/AgCl (3M) and a Pt foil were adopted as reference electrode and counter electrode, respectively.

The blueberry samples were digested by wet digestion method. The dried and crushed blueberry samples were weighed 0.25 g, with 12 mL of a mixture of concentrated nitric acid and perchloric acid added. The samples were placed in a 100 mL Kjeldahl flask with a funnel and glass beads overnight and cooked on a temperature-controlled digestion oven until the digestion was complete. Deionized water was fixed to 25 mL for the measurements.

3. RESULTS AND DISCUSSION

Figure 1A shows that the NC material has a uniform microscopic particle distribution and forms a dense structure. The nitrogen-doped carbon spheres are solid structures with smooth surfaces and no impurities. There are about 100 nitrogen-doped carbon spheres with a diameter of about 300 nm (Figure 1B). The surface functional groups of NC were recorded by FTIR. The broad band around 3000-3400 cm^{-1} can be assigned to the νO —H and νN —H stretching vibration, while the peaks at 1708 cm^{-1} were

corresponded to νC =O vibration. δN —H and νC —N stretching brands of amino groups located at 1607 cm^{-1} and 1374 cm^{-1}, respectively.

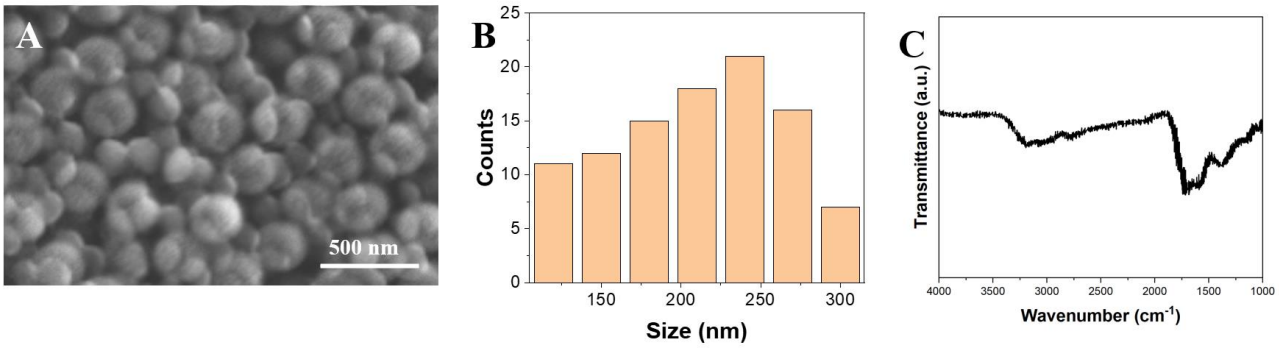

Figure 1. (A) SEM image, (B) size distribution and (C) FTIR of NC.

Figure 2A presents the electrochemical characterization of the GCE and NC/GCE electrodes with the elecctrochemical impedance spectroscopy. The impedance of the system was measured by applying a small amplitude sinusoidal interference signal to the working electrode to determine the ability of the electrode to conduct electrons. The impedance of the system was measured in a 10 mM $K_3[Fe(CN)_6]$ solution (containing 0.1 M KCl), which was used to characterize the impedance of both electrodes, and the magnitude of the resistance at the electrode surface was measured. The surface resistance of the electrode can be derived from the diameter of the semicircular part. It can be seen that the surface resistance of NC/GCE electrode is 385.42 Ω, while the surface resistance of GCE electrode is 833.61 Ω, which is 2.2 times higher than that of NC/GCE, which reveals that the introduction of NC material has the effect of reducing the resistance of the electrode surface and accelerating the electron transfer.

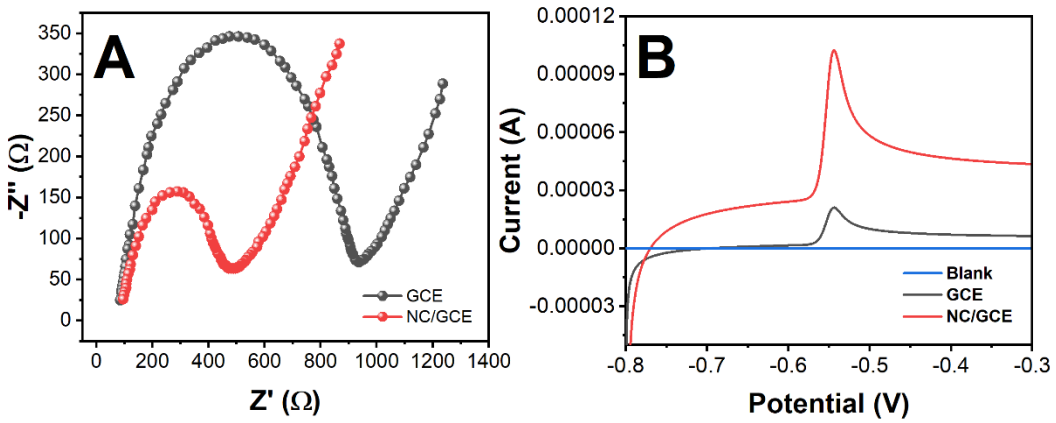

Figure 2. (A) EIS of GCE and NC/GCE in 10 mM $K_3[Fe(CN)_6]$ solution (containing 0.1 M KCl). (B) The electrochemical behavior of Pb^{2+} (10-5 M) on NC/GCE、GCE and blank scan.

Figure 2B shows the detection of Pb^{2+} ions at 10^{-5} M by GCE and NC/GCE. The NC/GCE blank scan to compare the electrochemical behavior of Pb^{2+} on the surface of both electrodes is also included in the figure. As shown in Figure 2B, the blank detection signal is almost zero, which indicates that the signals obtained by both sensors are for Pb^{2+}. The peak current I_p of the electrode reached 102.1 μA. The results show that the response signal of the modified NC/GCE electrode to Pb^{2+} is stronger than that of the bare GCE, indicating that the NCs material has a significant sensitizing effect on the Pb^{2+} detection signal, the reason for which is the formation of reactive adsorbed OH species that influence the kinetics of the reaction [41–44]. This study focuses on the sensors that are capable of directly detecting the Pb ions, thus an enhancement of the signal is necessary to determine the sub-nanomolar Pb concentration, since the amounts of free Pb^{2+} cations are lower at higher pH, due to their lower solubility, as chlorocomplexes and lead hydroxide are formed. For this purpose, the electrode surfaces were modified with NC, to improve the performance conditions of the GCE for heavy metal trace determination.

Since the peak position of lead ions in electrochemical detection experiments is around 0.55 V, it needs to be included in the initial and termination potentials. Given that only the post-oxidation dissolution peak needs to be shown in the differential pulse dissolution voltammogram, the initial potential is -0.8 V and the termination potential is -0.3 V.

The effect of potential increments was investigated in the range of 0.001 to 0.006 V on the electrochemical detection of lead. Figure 3A shows the results of the electrochemical detection at different potential increments. It can be noted that the peak current of lead shows a trend of increasing and then decreasing, with the increase of potential increment. In the range of 0.001-0.005 V, the peak current increases with the potential increment, whereas in the potential increment range of 0.005-0.006 V, the peak current decreases with the increase of potential increment. The peak current reaches the maximum at a potential increment of 0.005V. The final value of the potential increment was chosen as 0.005V.

The effect of pulse amplitude was investigated on the electrochemical detection of lead in the range of 0.01-0.1 V. Figure 3B shows the electrochemical detection results of lead at different pulse amplitudes, in which the peak current shows a trend of increasing and then decreasing, with the increase of pulse amplitude. In the range of 0.01 to 0.04 V, the peak current increases with the increase of potential increment. In the range of potential increment 0.04-0.1 V, the peak current decreases with the increase of potential increment, and the peak shape becomes worse. The peak current is highest at a potential increment of 0.04 V.

The effect of pulse widths was studied in the range of 10-50 ms on the electrochemical detection results of lead. Figure 3C shows the electrochemical detection results of lead under different pulse width conditions, in which the peak current shows a trend of increasing and then decreasing, with the increase of pulse amplitude. At the pulse width of 20 ms, the peak current reaches the maximum and the peak shape is better.

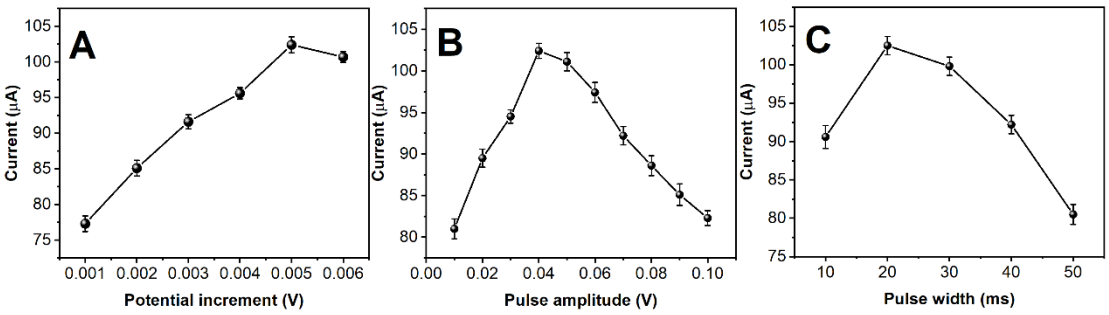

Figure 3. Effect of (A) potential increments, (B) pulse amplitude and (C) pulse width on electrochemical detection results.

The general heavy metal electrochemical detection enrichment potential is in the range of -1.0 to -1.4 V. In the case of an obvious oxidation peak of the substance to be measured, the accumulation at the negative potential and the oxidation phase scanning is necessary, which will be much more obvious than when it is not enriched. The effect of -0.8~-1.6V accumulation potential was investigated on the results of electrochemical detection of lead. Figure 4A shows the effect of different accumulation potentials on the experimental results. As the accumulation potential becomes more negative, the peak current value becomes larger, and the peak current is maximum when the accumulation potential reaches -1.3 V. Below -1.3 V, the peak current value decreases as the accumulation potential becomes more negative. It is possible that the more negative the accumulation potential is, the more difficult it is to reduce ions that are enriched on the electrode to interfere with the experiment.

The accumulation time is the time required to deposit the accumulation of the heavy metal ions to be measured onto the surface of the working electrode. In general, the longer the accumulation time is, the more heavy metals are deposited onto the working electrode surface and the higher the peak current is. The effect of the accumulation time in the range of 20-140 s on the heavy metal detection results was investigated, with the results shown in Figure 4B, which indicates that the growth trend is most stable and the peak height is relatively high when the accumulation time is 90s.

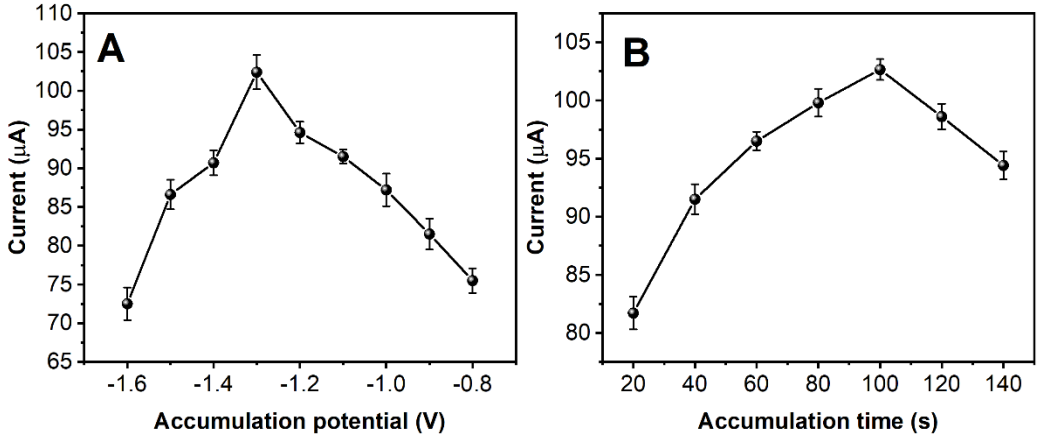

Figure 4. Effect of (A) accumulation potential and (B) accumulation time on electrochemical detection results.

After optimizing all parameters, the linear detection range of the sensor was investigated. As shown in Figure 5A, the current value increases with the concentration of lead ions. The linear detection curve of the NC/GCE sensor for lead ions is shown in Figure 5B, which presents that there is a positive linear relationship between NC/GCE in the range of 10 nM-4 μM. The detection limit was calculated as 1.05 nM. The extraordinary performance of the sensor occurred in two ways: 1) The high specific surface of the NC increased the effective electroactive surface area and improved the electrochemical response [45–47]. 2) The terminal amino groups at the edges of the NC increased adsorption sites of electrode surface to chelate lead cations [48].

As shown in Table 1, the detection limits of lead ions obtained in this work meet the requirements of low detection limits, indicating that NC/GCE can effectively detect lead ions and achieve the purpose of detecting trace lead ions.

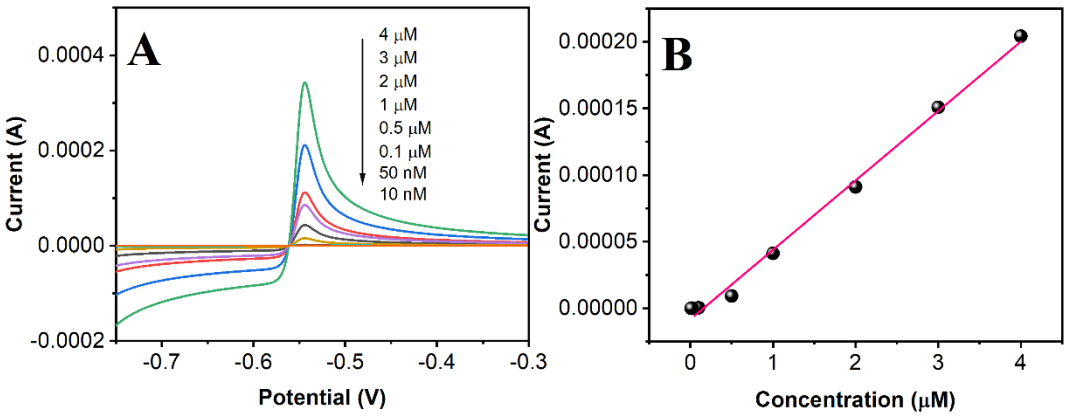

Figure 5. (A) DPV curves of the NC/GCE towards different concentrations of Pb^{2+}. (B) Plots of the current against the concentrations of Pb^{2+}.

Table 1. The detection limits of Pb^{2+} in different reference.

Sensor	LR	LOD	Reference
Bi/GCE	20 nM-150 nM	7.2 nM	[49]
ZnO/graphene/GCE	10 nM-600 nM	3.86 nM	[50]
Bi/GO/GCE	1 nM-200 nM	0.48 nM	[51]
Graphene/Au/GCE	5 nM-800 nM	2.65 nM	[52]
Graphene/Bi/GCE	1 nM-400 nM	0.8 nM	[53]
NC/GCE	10 nM-4 μM	1.05 nM	This work

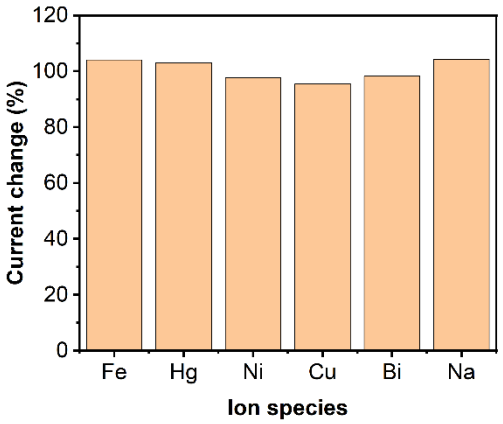

Figure 6. Selectivity performance of the NC/GCE for lead ions detection.

Selectivity is one of the most important parameters for electrochemical sensors. For the purpose of investigating the selectivity of NC/GCE, the sensor first detected the electrochemical signal of a solution with a concentration of 1 μM of lead ions, and added other metal ions with different concentrations as shown in Figure 6, which presents that NC/GCE has a good selectivity and can be used for the detection of complex systems.

Aiming to investigate the feasibility of NC/GCE in actual sample detection, a standard recovery method was adopted to detect the content of lead ions in blueberries. As shown in Table 2, the recovery of NC/GCE was within the range of 96.0-103.0%, indicating that NC/GCE can be used for the detection of blueberries with high accuracy.

Table 2. Determination of lead ions in blueberry samples with NC/GCE.

Sample	Added (μM)	Detected (μM)	Recovery rate (%)
1	0.00	0.00	-
2	0.50	0.48	96.00%
3	1.00	1.03	103.00%
4	2.00	2.05	102.50%

4. CONCLUSION

In conclusion, nitrogen-doped carbon nano was synthesized for the surface modification of GCE, and this NC/GCE has a very sensitive response to the detection of lead ions. After optimization, the NC/GCE can provide linear detection of lead ions in the range of 10 nM-4 μM. The detection limit was calculated to be 1.05 nM. This electrochemical sensor has excellent immunity to interference. The NC/GCE has been successfully adopted for the detection of lead ions in blueberries.

References

1. D.T. Altug, N.K. Kinayturk, B. Tunali, *Fresenius Environ. Bull.*, 29 (2020) 11266–11272.
2. H.F. Asiri, A.M. Idris, T.O. Said, T. Sahlabji, M.M. Alghamdi, A.A. El-Zahhar, A. El Nemr, *Fresenius Environ. Bull.*, 29 (2020) 615–625.
3. S. Barpete, P. Gupta, K.M. Khawar, S. Özcan, S. Kumar, *Fresenius Environ. Bull.*, 29 (2020) 2698–2706.
4. I. Bolat, A. Ikinci, *Fresenius Environ. Bull.*, 29 (2020) 1542–1549.
5. L. Fu, K. Xie, A. Wang, F. Lyu, J. Ge, L. Zhang, H. Zhang, W. Su, Y.-L. Hou, C. Zhou, C. Wang, S. Ruan, *Anal. Chim. Acta*, 1081 (2019) 51–58.
6. J. Zhou, Y. Zheng, J. Zhang, H. Karimi-Maleh, Y. Xu, Q. Zhou, L. Fu, W. Wu, *Anal. Lett.*, 53 (2020) 2517–2528.
7. L. Fu, W. Su, F. Chen, S. Zhao, H. Zhang, H. Karimi-Maleh, A. Yu, J. Yu, C.-T. Lin, *Bioelectrochemistry*, (2021) 107829.
8. H. Karimi-Maleh, Y. Orooji, F. Karimi, M. Alizadeh, M. Baghayeri, J. Rouhi, S. Tajik, H. Beitollahi, S. Agarwal, V.K. Gupta, *Biosens. Bioelectron.*, (2021) 113252.
9. H. Karimi-Maleh, M. Alizadeh, Y. Orooji, F. Karimi, M. Baghayeri, J. Rouhi, S. Tajik, H. Beitollahi, S. Agarwal, V.K. Gupta, S. Rajendran, S. Rostamnia, L. Fu, F. Saberi-Movahed, S. Malekmohammadi, *Ind. Eng. Chem. Res.*, 60 (2021) 816–823.
10. Z. Demir, D. Işık, *Fresenius Environ. Bull.*, 29 (2020) 1974–1987.
11. F. Kizilgeci, N.E.P. Mokhtari, A. Hossain, *Fresenius Environ. Bull.*, 29 (2020) 8592–8599.
12. Y. Xu, Y. Lu, P. Zhang, Y. Wang, Y. Zheng, L. Fu, H. Zhang, C.-T. Lin, A. Yu, *Bioelectrochemistry*, 133 (2020) 107455.
13. L. Fu, Y. Zheng, P. Zhang, H. Zhang, W. Zhuang, H. Zhang, A. Wang, W. Su, J. Yu, C.-T. Lin, *Biosens. Bioelectron.*, 120 (2018) 102–107.
14. M. Zhang, B. Pan, Y. Wang, X. Du, L. Fu, Y. Zheng, F. Chen, W. Wu, Q. Zhou, S. Ding, *ChemistrySelect*, 5 (2020) 5035–5040.
15. L. Fu, K. Xie, Y. Zheng, L. Zhang, W. Su, *Electronics*, 7 (2018) 15.
16. L. Fu, Y. Zheng, P. Zhang, J. Zhu, H. Zhang, L. Zhang, W. Su, *Electrochem. Commun.*, 92 (2018) 39–42.
17. W. Long, Y. Xie, H. Shi, J. Ying, J. Yang, Y. Huang, H. Zhang, L. Fu, *Fuller. Nanotub. Carbon Nanostructures*, 26 (2018) 856–862.
18. A. Özkan, *Fresenius Environ. Bull.*, 29 (2020) 143–151.
19. O. Ozbek, O. Gokdogan, M.F. Baran, *Fresenius Environ. Bull.*, 30 (2021) 1125–1133.
20. H. Karimi-Maleh, F. Karimi, S. Malekmohammadi, N. Zakariae, R. Esmaeili, S. Rostamnia, M.L. Yola, N. Atar, S. Movaghgharnezhad, S. Rajendran, A. Razmjou, Y. Orooji, S. Agarwal, V.K. Gupta, *J. Mol. Liq.*, 310 (2020) 113185.
21. H. Karimi-Maleh, B.G. Kumar, S. Rajendran, J. Qin, S. Vadivel, D. Durgalakshmi, F. Gracia, M. Soto-Moscoso, Y. Orooji, F. Karimi, *J. Mol. Liq.*, 314 (2020) 113588.
22. H. Karimi-Maleh, Y. Orooji, A. Ayati, S. Qanbari, B. Tanhaei, F. Karimi, M. Alizadeh, J. Rouhi, L. Fu, M. Sillanpää, *J. Mol. Liq.* (2020) 115062.
23. J. Li, S. Zhang, L. Zhang, Y. Zhang, H. Zhang, C. Zhang, X. Xuan, M. Wang, J. Zhang, Y. Yuan, *Front. Chem.*, 9 (2021) 339.
24. S. Yan, Y. Yue, L. Zeng, L. Su, M. Hao, W. Zhang, X. Wang, *Front. Chem.*, 9 (2021) 220.
25. T. Al-Gahouari, G. Bodkhe, P. Sayyad, N. Ingle, M. Mahadik, S.M. Shirsat, M. Deshmukh, N. Musahwar, M. Shirsat, *Front. Mater.*, 7 (2020) 68.
26. Z. Wu, J. Liu, M. Liang, H. Zheng, C. Zhu, Y. Wang, *Front. Chem.*, 9 (2021) 208.
27. D.A. Maya-Cano, S. Arango-Varela, G.A. Santa-Gonzalez, *Heliyon*, 7 (2021) e06297.
28. S. Rokayya, F. Jia, Y. Li, X. Nie, J. Xu, R. Han, H. Yu, S. Amanullah, M.M. Almatrafi, M. Helal, *LWT*, 137 (2021) 110422.

29. L. Jurgutis, A. Slepetiene, J. Volungevicius, K. Amaleviciute-Volunge, *Biomass Bioenergy*, 141 (2020) 105693.
30. G. Caposciutti, A. Baccioli, L. Ferrari, U. Desideri, *Energies*, 13 (2020) 743.
31. M. Silwamba, M. Ito, N. Hiroyoshi, C.B. Tabelin, R. Hashizume, T. Fukushima, I. Park, S. Jeon, T. Igarashi, T. Sato, *Metals*, 10 (2020) 531.
32. A. Boguslavsky, O. Gaskova, O. Naymushina, N. Popova, A. Safonov, *Appl. Geochem.*, 119 (2020) 104598.
33. J. Li, M. Li, D. Li, Q. Wen, Z. Chen, *Chemosphere*, 248 (2020) 126021.
34. Y. Lu, Y. Xu, H. Shi, P.Z.H. Zhang, L. Fu, *Int J Electrochem Sci*, 15 (2020) 758–764.
35. J. Cheng, Y. Li, J. Zhong, Z. Lu, G. Wang, M. Sun, Y. Jiang, P. Zou, X. Wang, Q. Zhao, *Chem. Eng. J.*, 398 (2020) 125664.
36. S. Vinoth, R. Ramaraj, A. Pandikumar, *Mater. Chem. Phys.*, 245 (2020) 122743.
37. C. Gu, Q. Wang, L. Zhang, P. Yang, Y. Xie, J. Fei, *Sens. Actuators B Chem.*, 305 (2020) 127478.
38. G. Muthusankar, R.K. Devi, G. Gopu, *Biosens. Bioelectron.*, 150 (2020) 111947.
39. R. Zhang, R. Jamal, Y. Ge, W. Zhang, Z. Yu, Y. Yan, Y. Liu, T. Abdiryim, *Carbon*, 161 (2020) 842–855.
40. H. Zhao, B. Liu, Y. Li, B. Li, H. Ma, S. Komarneni, *Ceram. Int.*, 46 (2020) 19713–19722.
41. F.E. Salih, A. Ouarzane, M. El Rhazi, *Arab. J. Chem.*, 10 (2017) 596–603.
42. Z. Dahaghin, P.A. Kilmartin, H.Z. Mousavi, *Food Chem.*, 303 (2020) 125374.
43. Y. Zheng, J. Zhu, L. Fu, Q. Liu, *Int J Electrochem Sci*, 15 (2020) 9622–9630.
44. Y. Zheng, H. Zhang, L. Fu, *Inorg. Nano-Met. Chem.*, 48 (2018) 449–453.
45. Y. Wang, G. Zhao, G. Zhang, Y. Zhang, H. Wang, W. Cao, T. Li, Q. Wei, *Sens. Actuators B Chem.*, 319 (2020) 128313.
46. T. Zhang, C. Gao, W. Huang, Y. Chen, Y. Wang, J. Wang, *Talanta*, 188 (2018) 578–583.
47. G. Liu, X. Yang, H. Zhang, L. Fu, *Int J Electrochem Sci*, 15 (2020) 5395–5403.
48. G. Chen, W. Bai, Y. Jin, J. Zheng, *Talanta*, 232 (2021) 122405.
49. A.F. Al-Ghamdi, *J. Taibah Univ. Sci.*, 8 (2014) 19–25.
50. W. Xiong, L. Zhou, S. Liu, *Chem. Eng. J.*, 284 (2016) 650–656.
51. D. Sun, Z. Sun, *J. Appl. Electrochem.*, 38 (2008) 1223–1227.
52. M.L. Yola, N. Atar, M.S. Qureshi, Z. Üstündağ, A.O. Solak, *Sens. Actuators B Chem.*, 171 (2012) 1207–1215.
53. C. Kokkinos, A. Economou, N.G. Goddard, P.R. Fielden, S.J. Baldock, *Talanta*, 153 (2016) 170–176.